International Journal of Innovative Research in Science, Engineering and Technology (IJIRSET)

| e-ISSN: 2319-8753, p-ISSN: 2320-6710| www.ijirset.com | Impact Factor: 7.512|

|| Volume 9, Issue 5, May 2020 ||

An Emerging Approach for Hyperspectral Image Mixed Noise Reduction Using CNN Deep Learning Algorithm

Mr.Yared Abera Ergu[1], Dr.S. Kother Mohideen[2]

Dean, School of Technology & Informatics, Ambo University, Woliso Campus, Ethiopia[1]

Professor, Department of Information System, Ambo University, Woliso Campus, Ethiopia[2]

ABSTRACT : In digital image processing, filtering noise to reconstruct a high quality image is an important work for further image processing such as object segmentation, detection, recognition and tracking .In this paper we deal with mixed noise reduction algorithm for Hyper spectral imagery (HSI). The Hyper spectral data cube is considered as a three order tensor that is able to jointly treat both spatial and spectral modes. This entire denoising process is based CNN model in deep learning for removing mixed noises in the Hyper spectral images. Our work involved in Neural Network training model to remove mixed noise such as Gaussian-Gaussian mixture, impulse noise and Gaussian-impulse noise from the HSI data. And also image denoise processed based on wavelet Domain . To solve the weighted rank-one approximation problem arisen from the proposed model, a new iterative scheme is given and the low rank approximation can be obtained by singular value decomposition(SVD) and we present a new weighting data fidelity function, which has the same minimize as the original likelihood functional but is much easier to optimize. The weighting function in the model can be determined by the CNN algorithm itself, and it plays a role of noise detection in terms of the different estimated noise parameters. Finally applied the Wavelet based high end threshold Neighsureshrink method. The experiment results shows that superior performance overcome the wiener filter and improved *K-SVD algorithm in terms of PSNR values.*

KEYWORDS: Hyper spectral image(HIS), K-SVD (Singular Value Decomposition) algorithm, CNN (Convolution Neural Network) , low rank approximation, Gaussian noise, Impulse noise, Mixed noise. Wavelet, PSNR(Peak Signal to Noise Ratio), PDF(Probability Density Function)

I. INTRODUCTION

The „Hyper" means „over" and refers to a the large number of measured wavelength bands. HSI are spectrally over determined, which means it provides ample spectral information to identify and distinguish spectrally unique materials. The development of hyper spectral remote sensing technology makes it possible to provide large amount of spatial and spectral information for image analysis application such as classification, immixing, sub pixel mapping and target detection[24]. However the acquired images are often distributed by radiometric noise such as sensor noise, photon noise calibration error, atmospheric scattering and absorption. The noise in these images can be categorized into two types: random noise and fixed–pattern noise. Fixed pattern noise is mostly due to calibration can be mitigated with suitable methods. In contrast, random noise cannot be removed entirely, due to its stochastic nature.

The traditional methods employ denoising algorithms such as singular value decomposition (SVD) and Wiener and wavelet filters, channel by channel. However these may lead to loss of the inter-dimensional information since they do not deal with the spatial and spectral information simultaneously .In recent years, some algorithm combine the spatial and spectral information for HSI noise reduction. A hybrid spatial spectral derivative domain wavelet shrinkage noise reduction (HSSNR) approach and spectral- spatial adaptive total variation model for hyper spectral image denoising was proposed.

In multi linear algebra, the HSI data cube can be considered as a three order tensor in which the spatial and spectral information are completely preserved. Examples of such approaches include multidimensional filtering based on tucker tensor decomposition. The multidimensional Wiener filtering (MWF) algorithm [13] is one of the Tucker based noise reduction which achieves simultaneous improvement in the image quality and classification accuracy. However this application may lead to information compression and loss of spatial details.

| e-ISSN: 2319-8753, p-ISSN: 2320-6710| www.ijirset.com | Impact Factor: 7.512|

|| Volume 9, Issue 5, May 2020 ||

In the rank-1 tensor decomposition (R1TD) algorithm [24], the input data cube is considered as three order tensor. Subsequently, is used to extract the signal-dominant component from the observed HSI data cube by sorting the Eigen values generated by tensor decomposition. The signal-dominant components are extracted from the observed data cube by sorting the weights of the rank-1tensor, and then they are reconstructed to produce the noise free image. In this work, we propose a general framework to adaptively detect and remove noise of different type, including Gaussian noise, impulse noise and more importantly, their mixture in the HSI data. The HSI data is considered as a three order tensor which treats.

The image undergoes tensor decomposition; later the modified K-SVD algorithm is applied to the tensors. We derive our model from the regularized maximum likelihood estimation (MLE) of the noise. Since the likelihood functional related to mixed noise is not easy to be optimized compared with the functional for a single Gaussian noise, a new functional with an additional variable is introduced. This new functional is easier to be optimized and has the same global minimize (or maximize) as the original likelihood functional. By minimizing the new functional, we obtain some weighted norms models, in which the weighting functions play the role of noise detectors. By integrating this with sparsity representation, our model can well restore images and textures corrupted by mixed noise[24].

To solve the weighted rank-one approximation problem arisen from the proposed model, a new iterative scheme is given and the low rank approximation can be obtained by singular value decomposition (SVD). Our method integrates sparse coding-dictionary learning, image reconstruction, noise clustering (detection), and parameters estimation into a four step algorithm. Each step needs to solve a minimization problem. Then these optimized tensors are separated as noise free tensor and noisy tensor. The noise free tensors are then combined to reconstruct the noise free image. The reconstruction is same as reverse of the tensor decomposition.

image collection, the local features were extracted and then by using the Adjustable surface normal overlap segmentation algorithm, they were clustered typically for content based image retrieval in the classification. The visual words which is called as the computer cluster centers and then form a codebook, which forms an indexing newly added images as a basis. The local features were extracted from the best fitting visual words and the local features were extracted and assigned. In the existing image collection, the new image is added. The local features in distribution, which indicates the local feature histogram over the former computed cluster, which serves as the new image for the computed cluster. Similar images were retrieved by using the CNN.

II. BRIEF REVIEW ABOUT HSI AND TENSORS

A. Spectral Image Analysis

To understand the advantages of hyper spectral imagery, it may help to first review some basic spectral remote sensing concepts. You may recall that each photon of light has a wavelength determined by its energy level. Light and other forms of electromagnetic radiation are commonly described in terms of their wavelengths. For example, visible light has wavelengths between 0.4 and 0.7 microns, while radio waves have wavelengths greater than about 30 cm (Fig. 1).Reflectance is the percentage of the light hitting a material that is then reflected by that material (as opposed to being absorbed or transmitted).

Some materials will reflect certain wavelengths of light, while other materials will absorb the same wavelengths. These patterns of reflectance and absorption across wavelengths can uniquely identify certain materials.

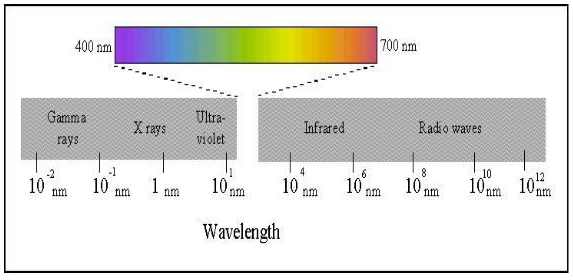

Fig 1 Electromagnetic Spectrum

B. Imaging Techniques

Depending on the number of spectral bands and wavelengths measured, an image is classified as a multispectral image when several wavelengths are measured and a hyperspectral image when a complete wavelength region, i.e., the whole spectrum, is measured for each spatial point. For example, a RGB image from a typical digital camera is a type of multispectral image that uses the light intensity at three specific wavelengths: red, green, and blue,

| e-ISSN: 2319-8753, p-ISSN: 2320-6710| www.ijirset.com | Impact Factor: 7.512|

|| Volume 9, Issue 5, May 2020 ||

to create an image in the visible region. The Fig 2 compares the optical information obtained by monochrome cameras, RGB cameras, and hyperspectral cameras[24].

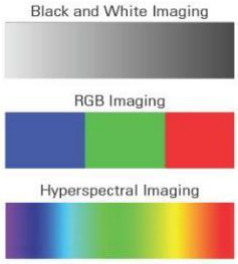

Fig 2 Differences in imaging

C. Imaging spectrometer

Hyperspectral images are produced by instruments called imaging spectrometers. The development of these complex sensors has involved the convergence of two related but distinct technologies: spectroscopy and the remote imaging of Earth and planetary surfaces

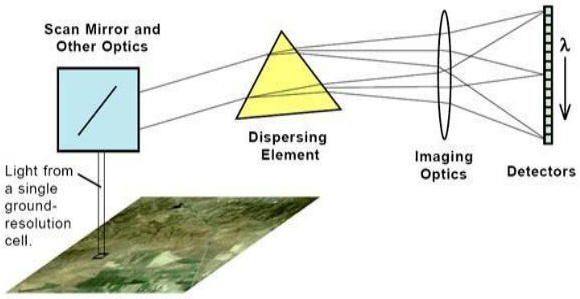

Fig 3 Imaging Spectrometer

Spectroscopy is the study of light that is emitted by or reflected from materials and its variation in energy with wavelength. As applied to the field of optical remote sensing, spectroscopy deals with the spectrum of sunlight that is diffusely reflected (scattered) by materials at the Earth‟s surface. Instruments called spectrometers (or spectroradiometers) are used to make ground-based or laboratory measurements of the light reflected from a test material. An optical dispersing element such as a grating or prism in the spectrometer splits this light into many narrow, adjacent wavelength bands and the energy in each band is measured by a separate detecto[24]r. By using hundreds or even thousands of detectors, spectrometers can make spectral measurements of bands as narrow as 0.01 micrometers over a wide wavelength range, typically at least 0.4 to 2.4 micrometers (visible through middle infrared wavelength ranges).

D. Tensor

A tensor, represented as is defined as a multidimensional array which is the higher-order equivalent of the vector (one-order tensor) and a matrix (two-order tensor). In this study, the HSI data cube is regarded as a three-order tensor in which modes1 and 2 represent the spatial modes and mode 3 denotes the spectral mode. Taking each vector to be in different mode, we can visualize the outer product of three vectors as follows,

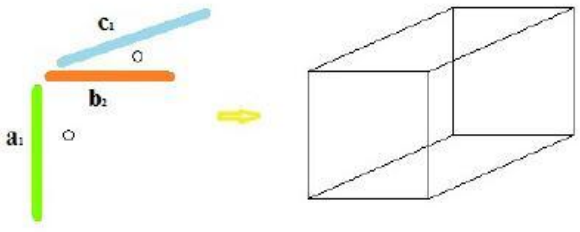

Fig 4 Tensor as the outer product of three vectors

| e-ISSN: 2319-8753, p-ISSN: 2320-6710| www.ijirset.com | Impact Factor: 7.512|

|| Volume 9, Issue 5, May 2020 ||

Mathematically, we can write the outer product of three vectors a; b; c as follows,

$$\begin{pmatrix} a_1 \\ a_2 \end{pmatrix} \circ \begin{pmatrix} b_1 \\ b_2 \end{pmatrix} \circ \begin{pmatrix} c_1 \\ c_2 \end{pmatrix} = \begin{matrix} a_1b_1c_2 & a_1b_2c_2 \\ a_2b_1c_2 & a_2b_2c_2 \end{matrix} \quad \begin{matrix} a_1b_1c_1 & a_1b_2c_1 \\ a_2b_1c_1 & a_2b_2c_1 \end{matrix}$$

We can see that the indexes of the entries in the resulting tensor.Tensor matricization reorders the elements of an N-order tensor into a matrix from a given mode. The n-mode matricization of X belongs to $R^{L1\times L2\times\ldots\times LN}$ is matnX belongs to $R^{Li\times(L1L2\ldots Ln-1\ Ln+1\ldots LN)}$, which is the ensemble of vectors in the n-mode obtained by keeping index Li fixed and varying the other indices. A visual illustration of tensor matricization is shown in Fig 5.

III. METHODOLOGY

The given HSI is taken as input to the system. This HSI image is read and displayed. Then the HSI image processed in the R1TD algorithm to provide the Rank-1 Tensor profiles.

A. HSI Image Reader

The Hyperspectral imaging (HSI) collects and process information from across the electromagnetic spectrum. Much as the human eye sees visible light in three bands (red, blue, green), spectral imaging divides the spectrum into many more bands. This technique of dividing images into bands can be extended before can be extended beyond the visibility. Hyper spectral sensors collect information as a set of "images". Each image represents a range of the electromagnetic spectrum and is also known as a spectral band. These „images" are then combined and form a three dimensional hyper spectral data cube for processing and analysis. This module is designed to read and visualize the HSI images.

The HSI data is considered as multiple images combined as a cube. Thus we have view each image in a well furnished manner. Each image ahs slice of images of different colors. This slice of image is not taken as a single color image for the calculation instead it is taken as whole cube called tensors.

Here, we denote O as the observed HSI data cube consisting of the signal-dominant component S and the additive noise component N. By extending the classic two-dimensional additive noise model, the tonsorial formulation is,

$$O = S + N \qquad (1)$$

In this model, the noise is assumed to be white, Gaussian and independent from signal.

B. Tensor Decomposition

In this module, we develop a new tensor decomposition which jointly treats both the spatial and spectral modes. The R1TD algorithm is applied to the tensor data input which takes into account both the spatial and spectral information of the hyper spectral data cube. The tensor decomposition is of the form CANDECOMP/PARAFAC decomposition (Canonical decomposition and parallel factor decomposition).

The tensor decomposition was first attempted by Hitchcock in 1927 and Eckert and Young in 1936. However it was not fully introduced until 1970 with the work of Harshman about the PARAFAC decomposition of Carroll and Chang about CANDECOMP. Both paper appeared in Psychometrical and explained the same decomposition. The CANDECMOP/PARAFAC is based on the fact that tensors can be rewritten as the sum of the several other tensors. Since the outer product of the three vectors gives a tensor as a result. We shall denote this tensor to be of rank 1 and we will use the term "rank 1 tensor" to denote tensors that can be written as the outer product of the vector triple. The CANDECOMP/PARAFAC decomposition rewrites a given tensor as a sum of several rank 1 tensors. Following the argument above, we define a tensor to be rank 2 if it can be expressed as the sum of two rank 1 tensors. Similarly, we define a tensor to be of rank 3 if it can be expressed as the sum of three rank 1 tensors. Thus the definition of a rank of a tensor T is the minimal number of rank 1 tensors that yield T as a linear combination.

Based on the definitions of the rank 1 tensor and vector outer product, tensor can be represented with the rank-1 tensor decomposition model: (rank-1 tensor in this model) on three modes, and M is the number of rank-1 tensors used to restore the whole tensor O. Considering as the weight value, the above implies that the HSI data is a linear combination of a sequence of rank-1 tensors. However, there is currently no straight forward solution to M or the so-called tensor rank. The rationale of this problem is explained as follows: The rank of a three order tensor is equivalent to the minimal number of triads necessary to describe the tensor.

| e-ISSN: 2319-8753, p-ISSN: 2320-6710| www.ijirset.com | Impact Factor: 7.512|

|| Volume 9, Issue 5, May 2020 ||

C. Improved K-SVD algorithm

We, solve the following with four sub-minimization problem.

Sparse Coding and Dictionary Learning:

The first minimization problem is Applying the alternating algorithm again to this sub problem, this problem can be split into two convex sub problems corresponding to the so-called sparse coding step and the dictionary learning step, respectively. Let $v1$, this problem can be split into two convex sub problems corresponding to the so-called sparse coding step and the dictionary learning step, respectively. Let $v1$ be an inner iteration number[24], then and can be obtained by solving the following two minimization problems iteratively:

$$r_l^{v+1} = \frac{<u_{\cdot,l}^{v+1},\mathbf{1}>+\lambda<\mathbf{M}u_{\cdot,l}^{v+1},\mathbf{1}>}{<\mathbf{1},\mathbf{1}>+\lambda<\mathbf{M}\mathbf{1},\mathbf{1}>}$$

$$(\sigma_l^2)^{v+1} = \frac{<u_{\cdot,l}^{v+1},(g-f^{v+1})\circ(g-f^{v+1})>}{<u_{\cdot,l}^{v+1},\mathbf{1}>+\lambda\sum_{i=1}^{N}<\mathbf{R}_i u_{\cdot,l}^{v+1},\mathbf{R}_i\mathbf{1}>} + \frac{\lambda\sum_{i=1}^{N}<\mathbf{R}_i u_{\cdot,l}^{v+1},(\mathbf{D}^{v+1}\alpha_{\cdot,i}^{v+1}-\mathbf{R}_i f^{v+1})\circ(\mathbf{D}^{v+1}\alpha_{\cdot,i}^{v+1}-\mathbf{R}_i f^{v+1})>}{<u_{\cdot,l}^{v+1},\mathbf{1}>+\lambda\sum_{i=1}^{N}<\mathbf{R}_i u_{\cdot,l}^{v+1},\mathbf{R}_i\mathbf{1}>}.$$

CNN DEEP LEARNING TECHNIQUE

A neural network is a system of interconnected Artificial "neurons" that exchange messages between each other. The connections have numeric weights that are tuned during the training process, so that a properly trained network will respond correctly when presented with an image or pattern to recognize[25]. The network consists of multiple layers of feature-detecting "neurons". Each layer has many neurons that respond to different combinations of inputs from the previous layers. Convolution Neural Network (CNN) is a deep learning technique. CNNs are used in variety of areas, including image and pattern recognition, speech recognition, natural language processing, and video analysis. There are a number of reasons that convolution neural networks are becoming important. In traditional models for pattern recognition, feature extractors are hand designed. In CNNs, the weights of the convolution layer being used for feature extraction as well as the fully connected layer being used for classification are determined during the training process[25]. The improved network structures of CNNs lead to savings in memory requirements and computation complexity requirements and, at the same time, give better performance for applications where the input has local correlation (e.g., image and speech).

- The training procedure of Algorithm CNN is described below:

Step 1: D is taken as input.

Step 2: For each image I_1^{tr} in D^{tr} of D compute the color features and they can be determined as F_{l,c_i}^{tr} for extracting the texture features, F_{l,T_j}^{tr} can be determined and for the shape features, F_{l,S_k}^{tr} can be determined, where i = 1,2,….n_c, j=1,2,…..n_T, k = 1, 2,…. n_s:

Step 3: For each image I_1^{tr} in D^{tr} of D each of n_d distance formulas is calculated for finding the distances of color features, texture features, and shape features for two different images I_1^{tr} and I_v^{tr} the distances calculation is given below:

$$d_{l,c_i}^{tr} = \left(F_{l,c_i}^{tr}, F_{v,c_i}^{tr}\right), d_{l,T_j}^{tr} = \left(F_{l,T_j}^{tr}, F_{l,T_j}^{tr}\right), and\ d_{l,s_k}^{tr} = (F_{l,S_k}^{tr}, F_{v,S_k}^{tr}),$$

Where I_v^{tr} indicates the v[th] image of the training set D^{tr} in D, l ≠v, l ,v ∈{1; 2….,m_{tr}}

Step 4: For D^{tr} in D, // GWO proceed for each epoch
For each solution k //for each parameter set, (Φ_k, w_k)
For each $I_1^{tr} \in D^{tr}$ //for all training images
call Image Retrieval (D, $n_g, \Phi_k, w_k, I_1^{tr}$)
Loop
compute the fitness for (Φ_k, w_k)which is the average of precision rates for each I_1^{tr}.
save parameters G best and P best which have the highest fitness during each epoch.
Loop
save G best in (Φ_0, w_0).
Loop

Step 5: Output (Φ_0, w_0), where

$\Phi_0 = F_{C_{i_0}}^{tr}, d_{C_0}^{tr}), \left(F_{T_{j_0}}^{tr}, d_{T_0}^{tr}\right), (F_{S_{k_0}}^{tr}, d_{S_0}^{tr})\}$

$w_0 = (w^C, w^T, w^S)$

For retrieving the images from the input image, '*Image Retrieval Algorithm'* is used .by setting the parameters and determines the extraction in the training phase for the query image and the Output of most similar images in an ascending can be determine.

Step 1: If $n_g = 1$ then $D^g = D^\Omega$ || D^Ω=D

Step 2: Set the parameters with Φ_k, W_k

Step 3: For a query image$I_q \in D^{te}$, three determined extraction methods in the training phase are utilized to compute three kinds of features $F_{q,c_{i_0}}^{te}, F_{q,T_{j_0}}^{te} and F_{q,S_{k_0}}^{te}$.

$$F_q^{te} = (F_{q,c_{i_0}}^{te}, F_{q,T_{j_0}}^{te}, F_{q,S_{k_0}}^{te})$$

Step 4: For each $D^{g,te}$ *in* D^g of D

$$d_{l,C_0}^g = \left(F_{l,C_{i_0}}^g, F_{q,C_{i_0}}\right), d_{l,T_0}^g = \left(F_{l,T_{j_0}}^g, F_{q,T_{j_0}}\right), and\ d_{l,S_0}^g = (F_{l,S_{k_0}}^g, F_{q,S_{k_0}})$$

Step 5: For each D^g in D

For each$I_l^g D^g$

Compute the similarities $\Delta_{l,q}^g$ between I_l^g and Iq using the following similarity function Δ (I_l^g, I_q),

$$\Delta_{l,q}^g = \Delta(I_l^g, I_q) = (w^C, w^T, w^S)(d_{l,C_0}^g, d_{l,T_0}^g, d_{l,S_0}^g)$$

Where t denotes the transpose operation for the vectors.

Step 6: Sort the similarities $\Delta_{l,q}^g$ by an ascending order.

Step 7: Output several most similar images in an ascending fashion.

$$\Delta_{l,q}^g = \Delta(I_l^g, I_q) = (w^C, w^T, w^S)(d_{l,C_0}^g, d_{l,T_0}^g, d_{l,S_0}^g)$$

The training phase of Algorithm 2 is determined, by taking the input for each subset.

Step 1: Input D.

Step 2: For each subset D^g in D

For each image $I_{l,}^{g,tr} D^{g,TR}$ of D^g

Compute three kinds of features, $F_{l,C_i}^{g,tr}$,$F_{l,T_j}^{g,tr}$, and $F_{l,S_k}^{g,tr}$

where i = 1, 2,…., n_c, j = 1,2,….,n_t ; k=1, 2,….,n_s.

Step 3: For each subset D^g in D

For each image $I_{l,}^{g,tr} D^{g,tr}$ of D^g each of n_d distance formulas is employed to

Compute distances of three kinds of features for two different images $I_{l,}^{g,tr}$and $I_{v,}^{g,tr}$,where $I_{v,}^{g,tr}$ indicates the vth image of the training set of the gth category in $D^{g,tr}$of D, l ≠v, l ,v ∈{1; 2….,$m_{g,tr}$}.Three distances can be computed by the following formulas.

$$d_{l,C_i}^{g,tr} = \left(F_{l,C_i}^{g,tr}, F_{v,C_i}^{g,tr}\right), d_{l,T_i}^{g,tr} = \left(F_{l,T_j}^{g,tr}, F_{v,T_j}^{g,tr}\right), and\ d_{l,S_k}^{g,tr} = (F_{l,S_k}^{g,tr}, F_{v,S_k}^{g,tr})$$

Step 4: For each $D^{g,tr}$ in D^g of D // GWO procedure

set (1/3,1/3,1/3) to (w^c, w^T, w^s).

For each epoch

For each solution k

For each $I_{l,}^{g,tr} \in D^{g,tr}$

call Image Retrieval ($D^g, I_{l,}^{g,tr}, n_g, w_k, \phi_k^g$),

Loop

compute the fitness for ϕ_k^g which is the average of precision rates for each $I_{l,}^{g,tr}$.save parameters.

Loop

save best in ϕ_k^g

Loop

| e-ISSN: 2319-8753, p-ISSN: 2320-6710| www.ijirset.com | Impact Factor: 7.512|

|| Volume 9, Issue 5, May 2020 ||

Step 5: Output Φ0,

where$\{\phi_o^g | g = 1,2, \dots, n_g\}$

Φ_0=$\{((F_{C_{i_0}}^{g,tr}, d_{C_0}^{g,tr}), \left(F_{T_{j_0}}^{g,tr}, d_{C_{i_0}}^{g,tr}\right), (F_{C_{i_0}}^{g,tr}), F_{C_{i_0}}^{g,tr}) | g = 1,2, \dots., n_g\}$.

D. Denoising

The signal dominant components are combined leaving the noise tensors to the noise free image. After the noise components are removed, the signal-dominant components are obtained by reconstructing the remaining noise free tensor.

Neighshrink

For each noisy wavelet coefficient $W_{i,j}$ to be shrinked, it incorporates a square neighbouring window B_{ij} centered at it. The neighbouring window size can be represented as LXL, where L is a positive odd number. The Neighshrink shrinkage formula can be represented as

$$S2 = \sum k, I\varepsilon B \quad W \quad 2$$

$$i, j \qquad\qquad i, j \quad kl \qquad (10)$$

$$\bar{A} \qquad i, j = Wi, j\ Bi, j$$

where □ *i, j* is the estimator of the unknown noiseless coefficient, and λ is the universal threshold. (g) is defined as (g) = max (g,0). Different wavelet coefficient subbands are shrinked independently, but the threshold λ and neighbouring window size L keep unchanged in all subbands. When $S_{i,j}^2$ summation has pixel indexes out of the wavelet subband range, the corresponding terms in the summation are omitted. The shortcoming of this method is that using the same universal threshold λ and neighbouring window size L in all subbands is suboptimal.

SureShrink

SureShrink is a thresholding technique in which adaptive threshold is applied to subband, a separate threshold is computed for each detail subband based upon SURE (Stein's unbiased estimator for risk), a method for estimating the loss in an unbiased fashion. The optimal λ and L of every subband should be data-driven and minimize the mean squared error (MSE) or risk of the corresponding subband. Fortunately, Stein has stated that the MSE can be estimated unbiasedly from the observed data. NeighShrink can be improved by determining an optimal threshold and neighbouring window size for every wavelet subband using the Stein's unbiased risk estimate (SURE). For ease of notation, the Nsnoisy wavelet coefficients from subband 's' can be arranged into the 1-D vector. Similarly, we combine

for almost any fixed estimator θ_S based on the data w_S, the expected

loss (i.e. risk) $E\left\{\left\|\bar{\theta}s-\theta\right\|_2^2\right\}$ can be estimated unbiasedly. Usually, the noise standard deviation σ is set at 1, and

then

$$E\left\{\left\|\bar{\theta}s-\theta\ s\right\|^2\right\} \quad -N_s+E\left\{\left\|g(w_s)\right\|^2\right\} \quad +2\nabla.g(w_s)\} \qquad (11)$$

Neighsureshrink

The quantity

$$SURE(w_S, \lambda, L) = N_S + \sum_n \left\|g_n(w_n)\right\|_2^2 + 2\sum \frac{\partial g_n}{n\ n} \qquad (12)$$

is an unbiased estimate of the risk on subband s where L is the neighbourhood window size (L is an odd number and greater than 1, for example, 3, 5, 7, 9, etc.): $E\left\{\left\|\bar{\theta}s-\theta\right\|_2^2\right\} = E\{SURE(w_s, \lambda, L\}$. Then, it can be choosen the threshold λ^s and neighbouring window size L^s on subband 's' which minimizes SURE(w_s, λ, L).

the Ns unknown noiseless coefficients from subband 's' into the corresponding 1-D vector. Stein shows that,

| e-ISSN: 2319-8753, p-ISSN: 2320-6710| www.ijirset.com | Impact Factor: 7.512|

|| Volume 9, Issue 5, May 2020 ||

IV. EXPERIMENTAL RESULTS

The proposed algorithm is applied in 3 set of HSI data. The HIS cannot be taken as an image itself. The values are to plotted as an image for our visualization. Thus a set of values of the received image is plotted as an image for our visualization. The values are plotted as an image for the original data and for the Denoised data. The original values are not plotted fully, only certain area shown for the visualization for a clear idea of the HSI image. The three images with their denoised output is shown in figure 6-8,

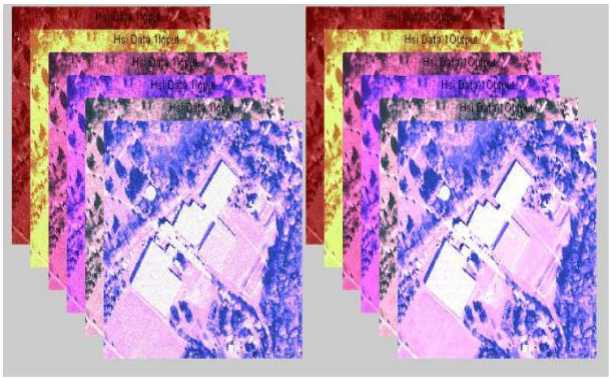

Fig 6 Data set 1 for HSI image visualization and the Denoised data set 1

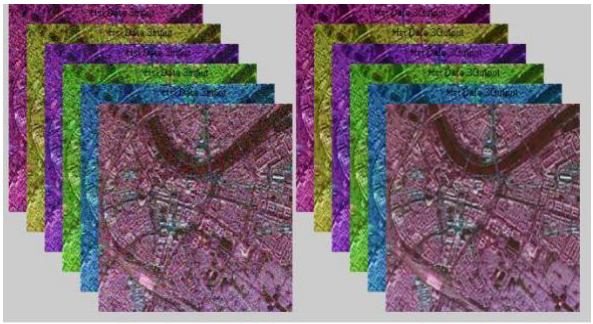

Fig 7 Data set 2 for HSI image visualization and the Denoised data set 2

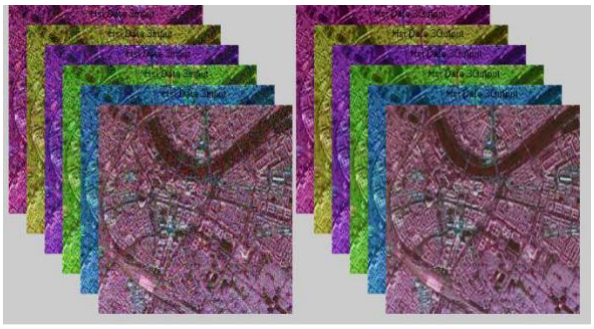

Fig 8 Data set 3 for HSI image visualization and the Denoised data set 3

To verify the effectiveness of the proposed algorithm, the proposed model is compared with several competitive methods: Spectral-Spatial Adaptive Total Variation (SSAHTV), Multidimensional Wiener Filtering (MWF) and Rank-1 Tensor Decomposition (R1TD). The algorithm SSAHTV [15] and MWF [13] may lead to loss of inter-dimensional information since the correlation between the spatial and spectral bands are not simultaneously considered. The application of a core tensor and n-mode tensor product may lead to information compression and loss of spatial details

| e-ISSN: 2319-8753, p-ISSN: 2320-6710| www.ijirset.com | Impact Factor: 7.512|

|| Volume 9, Issue 5, May 2020 ||

The R1TD [24] provides clear view than that of the other two but it deals with only Additive white and Gaussian noise.The proposed algorithm deals mixed noise like impulse, Gaussian-Gaussian, Gaussian-impulse. Also it provides a higher PSNR than that of the existing system.The PSNR is an engineering term for ratio between the maximum possible power of a signal and the power of corrupting noise that affects the fidelity of its representation. Because many signals have a very wide dynamic range, PSNR is usually expressed in terms of logarithmic decibel scale.The PSNR for the Existing System is compared with the proposed algorithm in the Table I. This comparison confirms that proposed method is has higher values than that of the existing systems. Also the existing system deals only with single noise whereas this deals with mixed.

PSNR COMPARISON FOR THE PROPOSED AND THE EXISTING SYSTEMS					
PSNR Values					
Band No	MWF	SSAHTV	R1TD	Improved K-SVD	CNN BASED
1	24.48	28.40	30.39	36.51	40.58
2	24.66	26.44	30.43	34.42	35.45
3	25.48	28.43	30.43	31.75	34.55
4	24.31	28.21	30.20	33.58	37.56
5	24.73	29.02	29.99	34.36	35.67
6	23.73	27.56	29.52	31.14	38.78

The graph is plotted with the PSNR values provided

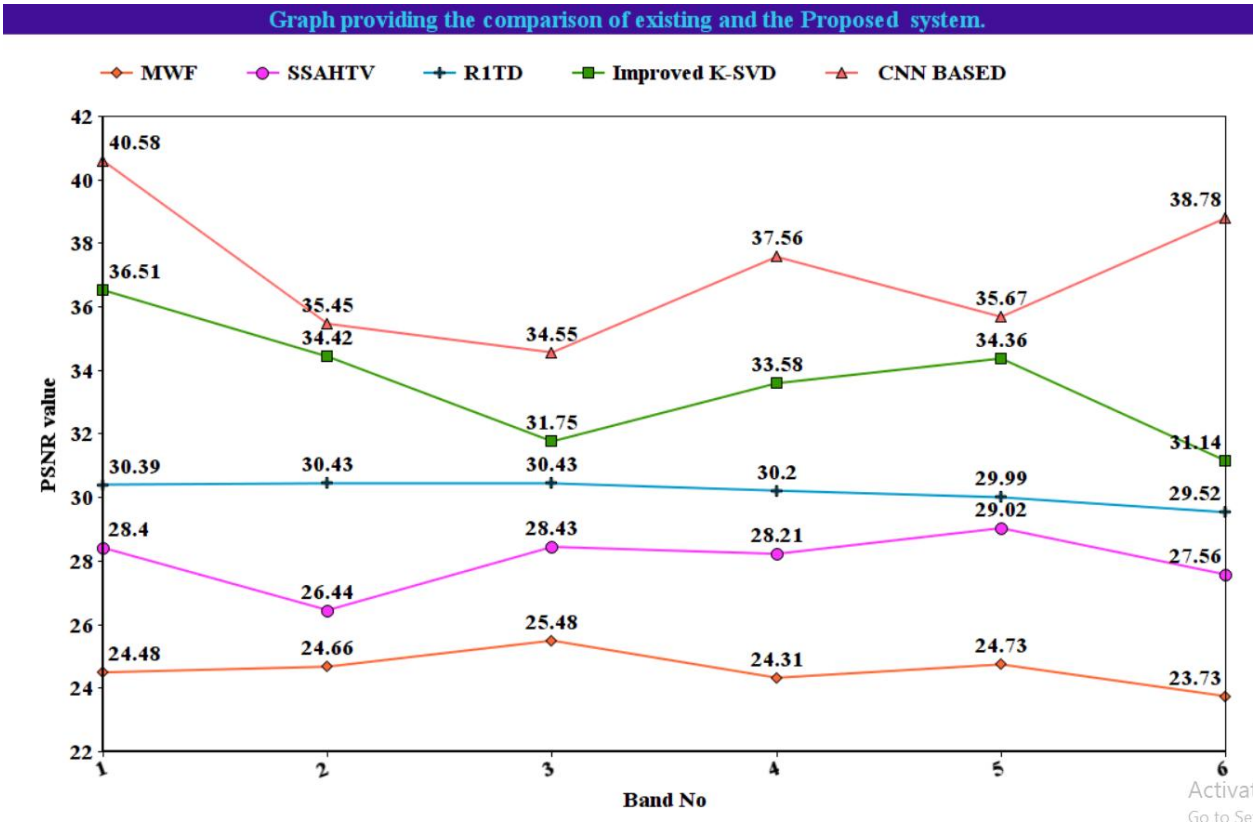

Fig 9 Graph providing the comparison of existing and the Proposed system

V. CONCLUSION

We provide a general framework to remove mixed noise using the PDF. By combing the sparsity regularization and dictionary learning techniques, a novel and efficient model is designed to remove mixed noise such as Gaussian-Gaussian mixture, impulse noise and Gaussian plus impulse noise. The weighting function in the model can be determined by the CNN algorithm itself, and it plays a role of noise detection in terms of the different estimated noise parameters. Finally applied the Wavelet based high end threshold Neighsureshrink method. The experiment results shows that superior performance overcome the wiener filter and improved K-SVD algorithm in terms of PSNR values. Also it considers both spatial and spectral views of the hyperspectral image thus provide data quality in terms of both visual inspection and image quality.

REFERENCES

[1] S. Ko and Y. Lee, "Center Weighted Median Filters and Their Applications to Image Enhancement," *IEEE Trans. Circuits Syst.*, vol. 38, no. 9, pp.984–993, Sep. 1991.
[2] H. Wang and R. Haddad, "Adaptive Median Filters: New Algorithms and Results," *IEEE Trans. Image Process.*, vol. 4, no. 4, pp. 499–502, Apr.1995.
[3] Bilmes. (1997). A Gentle Tutorial on the EM Algorithm and its Application to Parameter Estimation for Gaussian Mixture and Hidden Markov Models [Online]. Available: http://citeseerx.ist.psu.edu/viewdoc/summary?doi=10.1.1.28.613
[4] D. Landgrebe, "Hyperspectral Image Data Analysis," *IEEE Signal Process. Mag.*, 19 (1), 17–28, 2002.
[5] N. Srebro and T. Jaakkola, "Weighted low-rank approximations," *in Proc. 20th Int. Conf. Mach. Learn.*, pp. 720–727, 2003.
[6] R. Bro and H.A.L. Kiers, "A New Efficient Method for Determining the Number of Components in PARAFAC Models," *J. Chemometr.*, 17 (5), 274–286, 2003.
[7] H. Othman and S. E. Qian, "Noise Reduction of Hyperspectral Imagery Using Hybrid Spatial–Spectral Derivative-Domain Wavelet Shrinkage," *IEEE Trans. Geosci. Remote Sens.*, 44 (2), 397–408, 2006.
[8] M. Elad and M. Aharon, "Image Denoising via Learned Dictionaries and Sparse Representation," *in Proc. IEEE Comput. Vis. Pattern Recognit.*, pp. 895–900, Jun. 2006.
[9] M. Aharon, M. Elad, and A. Bruckstein, "The K-SVD: An Algorithm for Designing of Overcomplete Dictionaries for Sparse Representations," *IEEE Trans. Image Process.*, vol. 54, no. 11, pp. 4311–4322, Nov. 2006.
[10] M. Elad and M. Aharon, "Image Denoising via Sparse and Redundant Representations Over Learned Dictionaries," *IEEE Trans. Image Process.*, vol. 15, no. 12, pp. 3736–3745, Dec. 2006.
[11] J. Mairal, M. Elad, and G. Sapiro, "Sparse Representation for Color Image Restoration," *IEEE Trans. Image Process.*, vol. 17, no. 1, pp. 53–69, Jan. 2008.
[12] D. Letexier and S. Bourennane, "Noise Removal from Hyperspectral Images by Multidimensional Filtering," *IEEE Trans. Geosci. Remote Sens.*, 46 (7), 2061–2069, 2008.
[13] N. Acito, M, Diani, and G. Corsini, "Hyperspectral Signal Subspace Identification in the Presence of Rare Signal Components," *IEEE Trans. Geosci. Remote Sens.*, 48 (4), 1940–1954, 2010.
[14] A. Rovi., "Analysis of 2× 2 × 2 Tensors master‟s Thesis," 2010.
[15] E. Lopez-Rubio, "Restoration of Images Corrupted by Gaussian and Uniform Impulsive Noise," *Pattern Recognit.*, vol. 43, no. 5, pp. 1835–1846, 2010.
[16] J. Liu, H. Huang, Z. Huan, and H. Zhang, "Adaptive Variational Method for Restoring Color Images with High Density Impulse Noise," *Int. J.Comput. Vis.*, vol. 90, no. 2, pp. 131–149, 2010.
[17] Y. Xiao, T. Zeng, J. Yu, and M. K. Ng, "Restoration of Images Corrupted by Mixed Gaussian-Impulse Noise via l1-l0 Minimization," *Pattern Recognit.*, vol. 44, no. 8, pp. 1708–1720, Aug. 2011.
[18] A. Karami, M. Yazdi, and A. Z. Asli, "Noise Reduction of Hyperspectral Images Using Kernel Non-Negative Tucker Decomposition," *IEEE J. Sel. Top. Signal Process.*, 5(3), 487–493, 2011.
[19] S. Bourennane, C. Fossati, and A. Cailly, "Improvement of Target-Detection Algorithms Based on Adaptive Three-Dimensional Filtering," *IEEE Trans. Geosci. Remote Sens.*, 49 (4), 1383–1395, 2011.
[20] N. Acito, M. Diani, and G. Corsini, "Signal-Dependent Noise Modeling and Model Parameter Estimation in Hyperspectral Images," *IEEE Trans. Geosci. Remote Sens.*, 49 (8), 2957–2971, 2011a.
[21] N. Acito, M. Diani, and G. Corsini, "Subspace-Based Striping Noise Reduction in Hyperspectral Images," *IEEE Trans. Geosci. Remote Sens.* 49 (4), 1325–1342, 2011b.
[22] Q. Yuan, L. Zhang, and H. Shen, "Hyperspectral Image Denoising Employing a Spectral-Spatial Adaptive Total Variation Model," *IEEE Trans. Geosci. Remote Sens.*, 50 (10), 3660–3677, 2012.
[23] Brett W. Bader and Tamara G. Kolda, "MATLAB Tensor Classes for Fast Algorithm Prototyping.

| e-ISSN: 2319-8753, p-ISSN: 2320-6710| www.ijirset.com | Impact Factor: 7.512|

|| Volume 9, Issue 5, May 2020 ||

[24] P.Thazneem Fazila ,Dr.S.Kother Mohideen "A Novel Approach for Hyperspectral Image Noise Reduction Based on Improved K-SVD Algorithm" International Journal of Recent Development in Engineering and TechnologyWebsite: www.ijrdet.com (ISSN 2347 - 6435 (Online)), Volume 2, Special Issue 3, February 2014)

[25] K.M.Abubakker Sithik,Dr.S.Kother Mohideen," Computer Aided Diagnosis of Breast Nodule Detection Using Deep Learning Technique", International Journal of Psychosocial Rehabilitation, Vol. 24, Issue 05, 2020 ISSN: 1475-7192

[26] S.Kother Mohideen ,Dr.S.Arumuga Perumal,Dr.M.Mohamed Sathik,"Image Denoising Using Discrete Wavelet Transform" IJCSNS International Journal of Computer Science and Network Security, VOL.8 No.1, January 200

[27] Dr.S.Kother Mohideen "Denoising of Images Using Complex Multi avlet"International Journal of Advanced Scientific and Technical Research ,ISSUe 2,Volume1 February ,ISSN 2249-9954

[28] S. Shajun Nisha, P. Thazneem Fazila ,Dr. S. Kother Mohideen,"Hrperspectral Image Mixed Noise Reduction Based on Improved K- SVD Algorithm", International Journal of Research in Engineering Technology IJRET , Volume: 03 Special Issue: 07 |May-2014, eISSN: 2319-1163 | pISSN: 2321-7308